Surface activation for low temperature wafer fusion bonding by radicals produced in an oxygen discharge

Journal Item

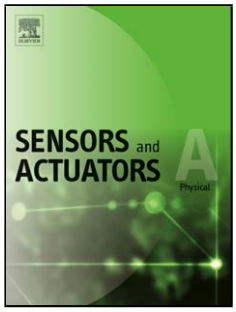

Title: Surface Activation for Low Temperature Wafer Fusion Bonding by Radicals Produced in an Oxygen Discharge

Authors: J. Kowal, T. Nixon, N. Aitken, N.St.J. Braithwaite

PII: S0924-4247(09)00393-8
DOI: doi:10.1016/j.sna.2009.08.018
Reference: SNA 6713

To appear in: *Sensors and Actuators A*

Received date: 28-1-2009
Revised date: 15-6-2009
Accepted date: 30-8-2009

Please cite this article as: J. Kowal, T. Nixon, N. Aitken, N.St.J. Braithwaite, Surface Activation for Low Temperature Wafer Fusion Bonding by Radicals Produced in an Oxygen Discharge, *Sensors and Actuators: A Physical* (2008), doi:10.1016/j.sna.2009.08.018

Surface Activation for Low Temperature Wafer Fusion Bonding by Radicals Produced in an Oxygen Discharge

J. Kowal[a*], T.Nixon[a], N. Aitken[b], and N. St. J. Braithwaite[a]

[a] The Open University, Walton Hall, Milton Keynes MK7 6AA, UK

[b] Applied Microengineering Limited, Unit 8, Library Avenue, Harwell International Business Centre, Didcot, Oxfordshire, OX11 0SG, UK

* corresponding author

Keywords: Wafer bonding; radical; activation; plasma; XPS; surface science; electron spectroscopy; fluorine; silicon

Abstract

A new method of exposing silicon/semiconductor wafers to a mixture of radicals is described, in which these species are generated in an oxygen-rich gas discharge confined between a concentric pair of annular mesh electrodes surrounding the wafers. This approach allows the wafer surfaces to be treated without damage from the energetic ions, strong electric fields, and high UV fluxes associated with direct treatment by exposure to gas discharge plasmas. The process is compared with direct oxygen plasma activation for its latitude with respect to treatment duration, effect on wafer surface roughness and bond strength. Wider process latitude and reduced surface roughening are obtained for treatment by radicals compared with direct plasma exposure. Comparative analysis of treated and untreated silicon surfaces by X-ray photoelectron spectroscopy indicate that traces of fluorine present on the wafer surface before treatment are removed with great efficiency by the process.

Introduction

Wafer bonding is ubiquitous in the semiconductor industry, whether it be applied to the manufacture of substrates for CMOS microelectronics, heterogeneous devices such as high brightness LEDs, or MEMS. High temperature fusion bonding, which involves treatment at temperatures in excess of 700°C, is well established for the manufacture of SOI substrates. However, where the wafers are of different materials or where at least one of the wafers contains other materials, such as for example metallization or patterned areas of different doping, exposure to such a large temperature cycle effectively destroys the devices.

Much work has therefore been focused on the development of low temperature bonding techniques for silicon wafers, where the term 'low temperature' means below 400°C – the upper limit on the temperature to which an aluminium metallization track on a silicon wafer can be taken without significant degradation of the film and the substrate interface. A more ambitious goal is to achieve full bond strength between silicon wafers below 200°C, which allows moderately temperature sensitive materials such as polymers, piezoelectric, and magnetic materials to pre-exist on the wafers. Yet another goal is to obtain good bonds without much exceeding room temperature. This allows bio-materials and other highly temperature sensitive materials to be used, and minimizes the thermal expansion mismatch between wafers of different materials. There are many examples [1-4] of devices that would benefit from the improvement of interlayer-free, low temperature silicon to silicon wafer bonding.

It has been shown [5] that increased bond strength (to about half the theoretical maximum bond energy density) between two oxidized silicon wafers is obtainable after their surfaces have been exposed to an oxygen plasma for 5 minutes prior to bonding, and after a post-bonding heat treatment at 200°C for 2h. Farrens et al. [6] showed that brief exposure to an oxygen plasma enables a variety of materials including homogeneous pairs of sapphire, silicon dioxide, silicon nitride, and gallium arsenide to be bonded together. High strength bonds between oxidized silicon wafers were achieved with a thermal cycle of less than 300°C.

Tagaki et al. [7] reported full-strength bonding between silicon wafers without the need for any heating at all using an Ar atom beam sputter etching process followed by bonding in-situ under vacuum. The study does not investigate the possible effects of damage from the high-energy Ar atoms, but since the process is known to etch silicon at a rate of approximately 4 nm per minute, it is reasonable to expect that the process does result in some degree of damage to the surface.

The system and method described in this paper is an attempt to avoid the shortcomings of the bonding techniques used to date.

Design and operation of the radical activation system using a gas discharge

Three principles govern the design of this radical generation system:

1. To protect the surfaces from strong electric fields, UV fluxes, and ion bombardment damage, the discharge that generates the radicals must be remote from the wafer surfaces.

2. To avoid the need for complex RF power supplies, the radical generator must operate under low voltage DC or 50-60 Hz AC excitation.

3. To ensure good treatment uniformity, the transport of the critical activating species to the wafer surfaces must occur sufficiently rapidly for the wafer activation to be rate-limited by the surface process rather than the concentration of species in the gas above the surface.

The design of the system, [8] is shown in Figure 1. The gas discharge is enclosed within an annular volume bounded by fine steel mesh walls at internal and external diameters of approximately 160 mm and 200 mm respectively. This is the radical generator. The mesh walls consist of perforated 0.1 mm thick stainless steel sheet containing a hexagonal array of 0.25 mm diameter circular holes creating a 22% open area. These electrodes are held at ground potential. A third mesh electrode of an intermediate diameter carries the electrical excitation, and the discharge is struck between this and the meshes to either side. Top and bottom, the radical generator is bounded by machinable glass-ceramic rings.

Thus, the first of the design principles is met: the radical generator ring lies beyond the outer diameter of the wafers, and the grounded meshes serve to create a field-free space around the wafers. Within the discharge region, the electric field is parallel to the plane of the annulus and therefore also to the wafer surfaces. This, and the field-free space surrounding the wafers, ensures that any ions carried past the mesh by their own momentum do not strike the wafer surfaces without first having undergone a collision in the gas. The pressure is sufficiently high also to ensure that any ions propelled past the mesh are rapidly thermalized. The flux of UV photons created within the discharge is

heavily attenuated as seen from the wafers; firstly by the small open area of the mesh, and secondly by the low angle of incidence with the wafer surfaces.

The second and third design principles are simultaneously met by choosing a combination of gas pressure and electrode spacing that allows the discharge to sustain itself at less than 300 V DC or AC, and using a pressure that allows the radicals to be transported to the centre of the wafer within a few seconds by diffusion, rather than viscous flow. For the purposes of estimating the rate of transport of species by diffusion, we can make some calculations based on ozone, the most massive radical the system is likely to produce. In focusing on ozone, we do not mean to suggest that we have identified this species as wholly or partly responsible for the activation effect: it has been chosen because it sets a lower bound on the rate at which species can be expected to diffuse within the vacuum chamber. According to Massman [9], the diffusion coefficient of ozone has never been measured in any gas, but his review of molecular diffusivities cites a number of models used to estimate its value in oxygen. He concludes that the best figure to use is 0.145 $cm^2\ s^{-1}$ at standard temperature and pressure. The diffusion coefficient is related to temperature and pressure by the expression

$$D_{(T,p)} = D_{(T_0\,,\,p_0)} \cdot (p_0/p) \cdot (T/T_0)^{1.8} \qquad (1)$$

At a pressure of 600 mTorr and a temperature of 300 K, this gives D for ozone in oxygen in the radical generator a value of 172 $cm^2\ s^{-1}$. The mean diffusion distance x after a time t is given by

$$x \approx (Dt)^{1/2} \qquad (2)$$

For a treatment time of one minute, *x* is approximately one metre. The distance between the inner diameter of the radical generator and the centre of the wafer is about 80 mm. It can therefore be assumed that after one minute of operation, ozone that has emerged from the inner mesh of the generator will be evenly dispersed throughout the volume between the wafers. Ozone is the most massive radical likely to be generated in the system, and since diffusion coefficient is approximately inversely proportional to the square root of the mass of the diffusing species [10], all the other radicals will be at least as well dispersed as the ozone. For example, according to Shibata [11], the diffusion coefficient for oxygen atoms in oxygen gas at 300 K and a pressure of 500 mTorr is 336 $cm^2 s^{-1}$, which equates to 280 $cm^2 s^{-1}$ at 600 mTorr.

Although ozone is generally regarded as an unstable molecule, at room temperature and low concentration, its rate of spontaneous decomposition into oxygen is very low. The dominant process responsible for the decomposition of ozone is chemical interaction with surfaces [12]. By this analysis, ozone can be assumed to be present at the wafer surface during the activation process, as can any lighter species whose lifetime exceeds a few tens of seconds.

Oxygen discharges have been extensively studied, and some of this work has included theoretical prediction and practical measurement of the concentrations of those radicals that are produced in the most significant quantities [13 - 15]. One species that has attracted much interest is the singlet delta g (SDO) metastable oxygen molecule. This is sufficiently long-lived and energetic to be an aggressive reagent on nearby surfaces. Other radicals include monatomic oxygen, which may also be in excited states. The process we have used employs a brief pump-down to a relatively high base pressure, and

no dwell time before the oxygen flow is introduced. This ensures that traces of nitrogen from the air, plus water vapour desorbed from surfaces in the chamber, will also contribute to the radicals produced in the discharge.

The electron density within the discharge region (i.e. in the space between the mesh electrodes) was measured using a hairpin probe [16], and found to be approximately 2.5×10^{16} m^{-3}. In the space between the wafers, the figure was below the detection limit of the method (5×10^{13} m^{-3}).

[Fig. 1]

Experimental

The radical activation process

The silicon wafers used throughout were prime 100 mm diameter <100> p-type wafers from Virginia Semiconductor. They were used as supplied; no pre-cleaning was done. Although all metrology was done under Class 100 clean-room conditions, it was found that wafer pairs bonded after any metrology operation always contained a higher percentage of unbonded area caused by particulate contamination. Therefore, metrology was carried out on representative samples from each batch, whilst other wafers were selected for bonding. The sample wafers were measured for bow and surface roughness using a Tencor P15 long-scan profilometer. Bow was found to lie within the range 0 to 20 μm total indicator reading and surface roughness was between 0.10 and 0.13 nm Ra.

Bonding was carried out in an AML-400 wafer bonder, adapted to house the radical generator. The process sequence was:

1. Load wafers onto top and bottom platens of AML-400
2. Pump down to a base pressure of 5×10^{-5} Torr
3. Introduce oxygen and maintain a pressure of 600 mTorr
4. Strike discharge and maintain a voltage of 300 V AC for 4 minutes
5. Switch off discharge and pump down to base pressure
6. Bond wafers in situ at base pressure
7. Vent chamber to air, remove wafers, and anneal at 200°C for 1h.

Process latitude

One of the important measures of the practicality of any wafer process is its latitude: the extent to which small changes in the process parameters affect the outcome. The process latitudes with respect to process duration for the radical activation and the oxygen plasma treatments were compared by carrying out a set of bonding experiments on wafers subjected to each treatment. The measure of bond quality was the crack opening test, developed by Maszara et al [17] to determine the bond energy. This was carried out on each wafer pair immediately after the post-contact annealing step.

The direct plasma treatment used was a capacitively coupled 13.56 MHz, 20 W oxygen plasma, at a pressure of 100 mTorr struck between the wafers, as shown in Figure 2.

[Fig. 2]

The radicals-only treatment applied was that described in the previous section. Figure 3 shows the variation of measured bond energy with exposure time for each surface treatment. From this graph, a standard exposure time of four minutes was determined as an optimum for the radicals-only treatment.

[Fig.3]

As another measure of the process latitude with respect to duration of exposure, surface roughness measurements were made of wafers subjected to each of the two treatments. For these measurements, an AFM, in tapping mode, was used. The results are shown in Table 1 of a wafer activated by the radical treatment (300 V, 110 mA, 600 mTorr), compared with another that had received the O_2 plasma treatment (50 W, 13.56 MHz, 65-67 mTorr). Treatment time in each case was increased from zero to 10 minutes, with roughness measurements being taken at 0, 2, 5, and 10 minutes total exposure.

[Table 1]

Whilst the differences between the two sets of results are not large, there appears to be a small upward trend in roughness for the plasma treatment, whereas there is no such indication for the radical treatment.

In view of the limited size of the data set, the investigation was continued with a larger number of wafers, including two control wafers not subjected to any treatment. An AFM used in tapping mode generates two data sets for each scan: the first is topographic data, a direct measurement of the vertical displacement of the AFM probe at each position on the surface as it comes into contact with it. The second is the phase data. This is information

reveals how the phase of the natural oscillation of the probe is shifted at each position a few nanometres over the surface by longer range interactions between the probe and the surface. This data set could therefore be expected to relate more directly to the wafer-surface-to-wafer-surface interactions involved in obtaining and maintaining the initial, low-strength contact bonding between wafers. The roughness figures obtained from the phase data are a convolution of the physical, topographic roughness of the surface, and something that might be called its 'chemical roughness', a measure of the strength of its interaction with the material of the AFM tip (in this case, also silicon). The results are shown in Figures 4 and 5.

[Fig. 4]

[Fig.5]

The striking thing about the data for both treatments is the strongly peaked trend in phase-mode roughness, and the mildly increasing or absent trend in topographic roughness with time. This confirms that the two types of measurement do indeed relate to different aspects of the surface. One plausible explanation is that the phase mode or 'chemical roughness' is highest near the beginning of the treatment because the density of sites on the surface that have become activated is still low. As time passes there is increasingly complete conversion of the surface to its activated form, and its phase mode roughness more closely approaches correspondence with the topographic measure. In addition, the slightly increasing topographic roughness for the plasma activated wafer could be an indication of the build-up of ion-induced surface damage.

There appears also to be greater random variability in the (topographic) roughness data for the plasma activated wafer. This aspect was further investigated by taking measurements at four positions on each wafer after a two minute exposure to each treatment. The results of this are shown in Table 2.

[Table 2]

Although again the data set is small, there is a marked increase in both the spread and mean value of roughness measured for the two wafers, with the plasma treated wafer showing the higher value in both cases. This may be a reflection of the different way in which the reactions occur in the two treatments. In radical activation, the reactive species arrive at the wafer surface through diffusion from their source beyond the edges of the wafers. The process time and gas kinetics together ensure that the distribution of radicals over the wafer surface is highly uniform. In contrast, the plasma process is chiefly driven by the electric field at the edges of the plasma. It is well known [18,19] from plasma assisted etching and deposition processes that features such as edges, wafer temperature variations, areas of different electrical properties, and variations in the topography of the treated surfaces all affect the rate of reaction.

XPS surface analysis of radical-treated silicon

A 100 mm wafer of a similar specification to those used for the wafer bonding tests was divided into 7 × 7mm dice. In order to prevent contamination of the polished surface by debris from the dicing process, the wafer was coated beforehand with positive photoresist. Immediately before subjecting individual dice to the activation process, this resist layer was stripped off using acetone, isopropyl alcohol and deionized water in

sequence, followed by drying in a helium flow. Experimental and control dice were treated in the same way (including placing them in the vacuum chamber), the only difference between treatments being whether the oxygen discharge was created while the die was in the vacuum chamber.

XPS measurements were performed using a Kratos XSAM 800 with a dual anode x-ray gun, a concentric hemispherical electron energy analyzer, and a channeltron detector. The source was a magnesium Kα x-ray beam with a resolution of 0.7 eV. In our experiments, performed at a base pressure of 2×10^{-9} mbar, the x-ray source power was 144 W at 12 kV to minimize sample heating. The angle of incidence of the x-ray beam with the sample normal was about 60°. XPS spectra were recorded in the fixed analyzer transmission (FAT) mode with a pass energy of 20 eV and with energy steps of 0.1 eV. The magnification of the analyzer in the fixed analyzer transmission (FAT) mode was selected to collect photoelectrons from an area of approximately 4 mm^2. To offset charging effects during x-ray irradiation of the samples, the energy axis of the XPS spectrum is usually shifted to make the C 1s binding energy line equal to 285 eV, a standard hydrocarbon energy of C-H and C-C bonds.

For any given silicon die, the elapsed time between the cessation of treatment and the first photoelectrons arriving at the channeltron electron detector in the XPS is approximately 15 minutes, of which the first five are spent in bringing the treatment chamber back up to atmospheric pressure, removing the die, placing it onto the spectrometer sample stub, and introducing it into the UHV chamber of the spectrometer via a load-lock system. The XPS spectrum of an untreated silicon surface is shown in

Figures 6 and 7. Figure 6 shows the entire spectrum. The most prominent features of this spectrum are labelled, and are consistent with what might be expected from a silicon surface that has been prepared in a laboratory atmosphere (as opposed to a UHV chamber). Thus, a significant peak due to the presence of carbon from hydrocarbons in the air is visible. By partially masking the surface, this carbon contamination has the effect of reducing the amplitudes of the peaks associated with silicon. A tiny feature, attributed to fluorine in trace quantities, is barely visible on the full spectrum. It is shown in Figure 7 at higher magnification, using 42 sweeps of the spectrometer collector to improve the signal to noise ratio.

[Figure 6]

[Figure 7]

A die subjected to 4 minutes of exposure to the radical activation process produced the spectrum shown in Figure 8. There are few noticeable differences between this and that of the untreated sample. At the energy resolution possible with this spectrometer (about 0.5 eV), no significant shift was observed in the position of any peak (which would have indicated a change to the chemical environment of the species producing that peak). The most obvious difference between the two spectra was the complete disappearance of the small fluorine 1s peak, situated at a binding energy of about 692 eV.

[Figure 8]

Figure 9 should be compared with Figure 7. It shows the effect on the region around the fluorine 1s peak when a silicon surface is given four minutes' exposure to the radical source.

[Figure 9]

In order to control for the possibility that any small sample-to-sample variation in the duration of exposure to X-rays during the collection of the spectrum was a factor in the observed data, we monitored the amplitude of a fluorine peak on a representative untreated silicon sample by gathering a series of spectra over an extended period of time (8 hours). The fluorine peak diminished in amplitude by 75% over this interval. This showed an effect that could be attributed to the passage of time in the environment of the XPS chamber under X-ray illumination. Nevertheless this is not sufficiently strong to account for the data we obtained, since the longest exposure during analysis was of the order of 15 minutes.

Bond quality

Scanning acoustic microscopic examination of the bonded wafer pairs showed little evidence of micro-void formation before post-bonding heat treatment (Figure 10). Even after treatment at 250°C, the extent of growth of existing voids and formation of new ones was slight (Figure 11). However, post-bonding heat treatment at 400°C showed increasing evidence of void growth and new void formation (Figure12).

The development of voids after low temperature annealing has been described previously [20], and is considered to be caused chiefly by the nucleation of interfacial water, some of which pre-exists in the form of several monolayers of adsorbed water, and some of which is formed during the polymerization of silanol bonds to Si-O-Si across the wafers. In addition, the desorption of adsorbed hydrocarbon contamination may contribute to the formation of interfacial voids.

[Figure 10]

[Figure 11]

[Figure 12]

The tendency of the interfacial voids observed in the present work to increase in size and number with increasing annealing temperature (at least up to 400°C) is consistent with the literature. We can therefore state that the process we have described does not offer an improvement in this respect, but neither are the results any worse than the norm for wafer bonding within this temperature range.

Discussion

Although the new process described here appears to work, in that wafers bonded after having been subjected to it exhibit full bond strength after annealing at a temperature of only 200°C for an hour, many questions remain about the process. The two most fundamental are: "Which precisely are the key species involved in the activation process?" and: "What is the nature of the resulting change to the wafer surface that gives it its enhanced ability to bond to a similar surface?"

The XPS results fail to reveal that the process alters the silicon surface much except for the elimination of fluorine – though even this was initially present only in a very low concentration. How or whether the removal of these traces of fluorine is important in the activation of the wafers is not clear. Hydrogen bonding can also occur between fluorine attached to a silicon surface and hydrogen atoms on nearby water molecules that can form a bridge to the surface of the other wafer [21]. If the strength of these hydrogen

bonds were found to be much lower than those between surface oxygen and nearby water molecules, then it could be argued that removing fluorine from sites on the wafer surface makes these available for occupation by oxygen or OH groups which could then form stronger hydrogen bonds. However, the opposite appears to be the case: the O-H ····· F hydrogen bond (in solution) has an enthalpy of 99 kJ mol^{-1}, compared with 10 kJ mol^{-1} for the aqueous O-H ····· O-H hydrogen bond. If the presence of the fluorine has a negative effect on wafer bond strength, another cause must therefore be identified. Such an explanation might invoke the weakening of Si-Si back bonds caused by the attachment of F to the surface Si atom [22].

It is also possible that the fate of the fluorine on the surface has only a minor effect on the bonding, and that some other phenomenon underlies the effect, undetected by our XPS measurements.

The XPS evidence also does not show that the process works by the cleaning off of hydrocarbon contamination: the carbon peaks are roughly of equal size on the treated and untreated samples. The possibility remains, however, that the radicals have created high-energy metastable states on the surface, without major changes to the chemical composition. Radicals such as O, O_3 and singlet delta g O_2 all carry sufficient energy to interact with the surface. It is worth bearing in mind that UV photons may also contribute energy to the silicon surface, since the process does not entirely shield the wafers from UV generated in the discharge.

Conclusion

We have demonstrated a new method of activating the surfaces of silicon wafers that allows them to be bonded to one another after activation without having to open the chamber, and without exposing them to the electric fields, intense UV radiation, and ion bombardment associated with plasma treatment; and also without the need for the high temperature annealing of conventional fusion bonding. The physical arrangement of the radical generator is such that no part of it encroaches into the space between the wafers, and this allows for a simple installation into an existing aligner-bonder, such as the AML-400 series machine used for these experiments. We have shown that the process has wide latitude with respect to treatment duration compared with a more conventional activation using a full exposure to an oxygen plasma.

It is important to realize, however, that the short time that elapses between loading the wafers into the chamber and commencing treatment means that whatever treatment is applied, the gas used is a mixture of oxygen and significant quantities of water vapour, as well as traces of air. This means that the ions and radicals created are derived not purely from oxygen, but also from water and nitrogen.

Acknowledgements

The authors gratefully acknowledge the UK Department for Trade and Industry's Micro and Nano-Technologies Initiative for their financial support.

References

1 W. Ma, G. Li, Y. Zohar and M. Wong, Fabrication and packaging of inertia micro-switch using low-temperature photo-resist molded metal-electroplating technology, Sens. Actuators A, 111 (1) (2004) 63 70.

2 A. Manz, N. Graber and H. M. Widmer, Miniaturized total chemical analysis systems: A novel concept for chemical sensing, Sens. Actuators B, 1 (1990) 244 248.

3 R. Brigel, M. Ashauer, A. Ashauer, H. Sandmeier and W. Lang, Anisotropic conductive adhesion of microsensors applied in the instance of a low pressure sensor, Sens. Actuators A, 97-98 (2002) 323 328.

4 U. Mescheder and S. Majer, Micromechanical inclinometer, Sens. Actuators A, 60, (1997) 134-138.

5 D. Pasquariello, C. Hedlund and K. Hjort, Oxidation and induced damage in oxygen plasma in situ wafer bonding, J. Electrochem. Soc., 147 (7) (2000) 2699 2703.

6 S. N. Farrens, J. R. Dekker, J. K. Smith, and B.E. Roberds, Chemical free room temperature wafer to wafer direct bonding, J. Electrochem. Soc., 142 (11) (1995) 3949 3955.

7 H. Takagi, R. Maeda, T. R.Chung and T. Suga, Low-temperature direct bonding of silicon and silicon dioxide by the surface activation method, Sens. Actuators A, 70 (1998) 164 170.

8 N. St. J. Braithwaite, J. Al-Kuzee and J. Kowal, Semiconductor Bonding Techniques, Patent application number GB0609167.2 (2006).

9 W. J. Massman, A review of the molecular diffusivities of H_2O, CO_2, CH_4, CO, O_3, SO_2, NH_3, N_2O, NO, and NO_2 in air, O_2 and N_2 near STP, Atmospheric Environment, 32 (6) (1998) 1111 1127.

10 E. H. Kennard, Kinetic Theory of Gases, McGraw-Hill, New York, 1938, p. 193.

11 M. Shibata, N. Nakano and T. Makabe, O_2 rf discharge structure in parallel plates reactor at 13.56 MHz for material processing, J. Appl. Phys., 77 (12) (1995) 6181 6188.

12 C. J. Weschler, Ozone in indoor environments: Concentration and chemistry, Indoor Air, 10 (4) (2000) 269 288.

13 A. A. Shepelenko, Estimates of maximal concentrations of singlet delta oxygen in a DC discharge, High Temperature, 45 (4) (2007) 439 445

14 A. P. Napartovich, A. A. Deryugin and I. V. Kochetov, Discharge production of the singlet delta oxygen for an iodine laser, J. Phys. D: Appl. Phys. 34 (2001) 1827 1833

15 C. M. Ferriera and G. Gousset, A consistent model of the low-pressure oxygen positive column, J. Phys. D: Appl. Phys. 24 (1991) 775 778

16 R. B. Piejak, J. Al-Kuzee and N. St. J. Braithwaite, Hairpin resonator probe measurements in RF plasmas, Plasma Sources Science and Technology, 14 (4) (2005) 734 743.

17 W. P. Maszara, G. Goetz, A. Caviglia and J. B. McKitterick, Bonding of silicon wafers for silicon-on-insulator, J. Appl. Phys., 64 (10) (1988) 4943 4950.

18 D. Tretheway, and E. S. Aydil, Modeling of heat transport and wafer heating effects during plasma etching, J. Electrochem. Soc., 143 (11) (1996) 3674 3680.

19 T. Brozek, X. Li, F. Preuninger, Y. D. Chan, and C. R. Viswanathan, Assessment of uniform and non-uniform damage in plasma etched submicron transistors, Proc. Int. Symp. on VLSI Technology, Systems, and Applications, Taipei, Taiwan ROC, May 31 – June 2, 1995, pp. 53 56.

20 Q.Y. Tong and U. Gösele, Semiconductor wafer bonding: science and technology, Wiley, New York, 1999

21 Q.Y. Tong, T.H. Lee, U. Gösele, M. Reiche, J. Ramm and E. Beck, The role of surface chemistry in bonding of standard silicon wafers, J. Electrochem. Soc., 144 (1) (1997) 384 389.

22 R.Q. Zhang, Y.L. Zhao and B.K. Teo, Fluorination-induced back-bond weakening and hydrogen passivation on HF-etched Si surfaces, Phys. Rev. B, 69 (12) (2004) 125319 125326.

Tables

Table 1. Surface roughness of silicon wafers after different exposure times

Exposure Time / min	Roughness Sa (nm) Oxygen plasma	Roughness Sa (nm) Radicals only
0	0.12	0.13
2	0.16	0.13
2	0.13	0.14
5	0.40	0.13
5	0.22	0.15
10	0.18	0.11
10	0.18	0.13

Table 2. Comparison of activation uniformity for radical and for plasma activation

Wafer position	Radical activation (2 minute exposure) Ra as measured by AFM (nm)	Oxygen plasma activation (2 minute exposure) Ra as measured by AFM (nm)
A	0.11	0.28
B	0.11	0.11
C	0.09	0.18
D	0.08	0.10
Std. deviation	0.01	0.08
Range	0.03	0.18
Mean value	0.10	0.17

Figure Captions

Figure 1. Cross-sectional view of the annular radical generator. The wafer platens and vacuum chamber are also shown. The chamber volume is approximately 22 litres.

Figure 2. Cross-section of the arrangement for plasma pre-treatment of wafers using direct exposure to a 13.56 MHz capacitively coupled oxygen plasma.

Figure 3. Bond energy versus duration of activation step for silicon-silicon after annealing at 200°C, as measured by the crack opening method.

A Oxygen plasma activated B Radical activated

Figure 4. Time evolution of phase mode and topographic roughness of oxygen plasma activated wafer.

Figure 5. Time evolution of phase mode and topographic roughness of radical activated wafer.

Figure 6. XPS wide spectrum of an untreated silicon surface

Figure 7. XPS spectrum of the region around the fluorine peak for an untreated silicon surface

Figure 8. XPS wide spectrum of a silicon surface after a 4 minute radical treatment

Figure 9. XPS spectrum of the region around the fluorine peak for a silicon surface after a 4 minute radical treatment.

Figure 10. Acoustic microscope image of a radical activated silicon wafer pair after bonding at 200°C, prior to annealing

Figure 11. Acoustic microscope image of wafer pair of Figure 11 after annealing for 1 hour at 250°C

Figure 12. Acoustic microscope image of a radical activated silicon wafer pair after annealing for 1 hour at 400°C

Biographies of authors

Jan Kowal graduated with a BSc in Physics at Imperial College in 1981 and has an MSc in Biophysics and Bioengineering. After stints as an engineer at GEC and at Fulmer Research, he co-founded Applied Microengineering, where he worked on various projects including the development of an anodic bonder. Since 2002 he has been a lecturer in Nanotechnology at the Open University.

Tony Nixon gained a BSc in Physics in 1989 from the University of York. In 1993 he was awarded a D.Phil. for his thesis on ion induced Auger spectroscopy. Between 1994 and 2000 Tony was a Staff Tutor in the Technology Faculty of the Open University. He is now a Senior Lecturer in Information Systems in the Faculty of Mathematics Computing and Technology and has a particular research interest in surface science and in particular electron spectroscopy.

Nick Aitken graduated from Durham University in 1999 with a BSc degree in Applied Physics and an MSc by research in II-VI semiconductor crystal growth. He has subsequently worked on various thin film and silicon wafer fabrication projects. Nick joined AML in 2002 as an Applications Engineer.

Nicholas Braithwaite earned his BSc degree in Physics from UMIST in 1976, followed by an MSc and a DPhil at Oxford University. He is a Fellow of the Institute of Physics. Professor Braithwaite currently heads the Department of Physics and Astronomy at the Open University. His main research interest is in the physics and applications of technological plasmas.

Figure 1

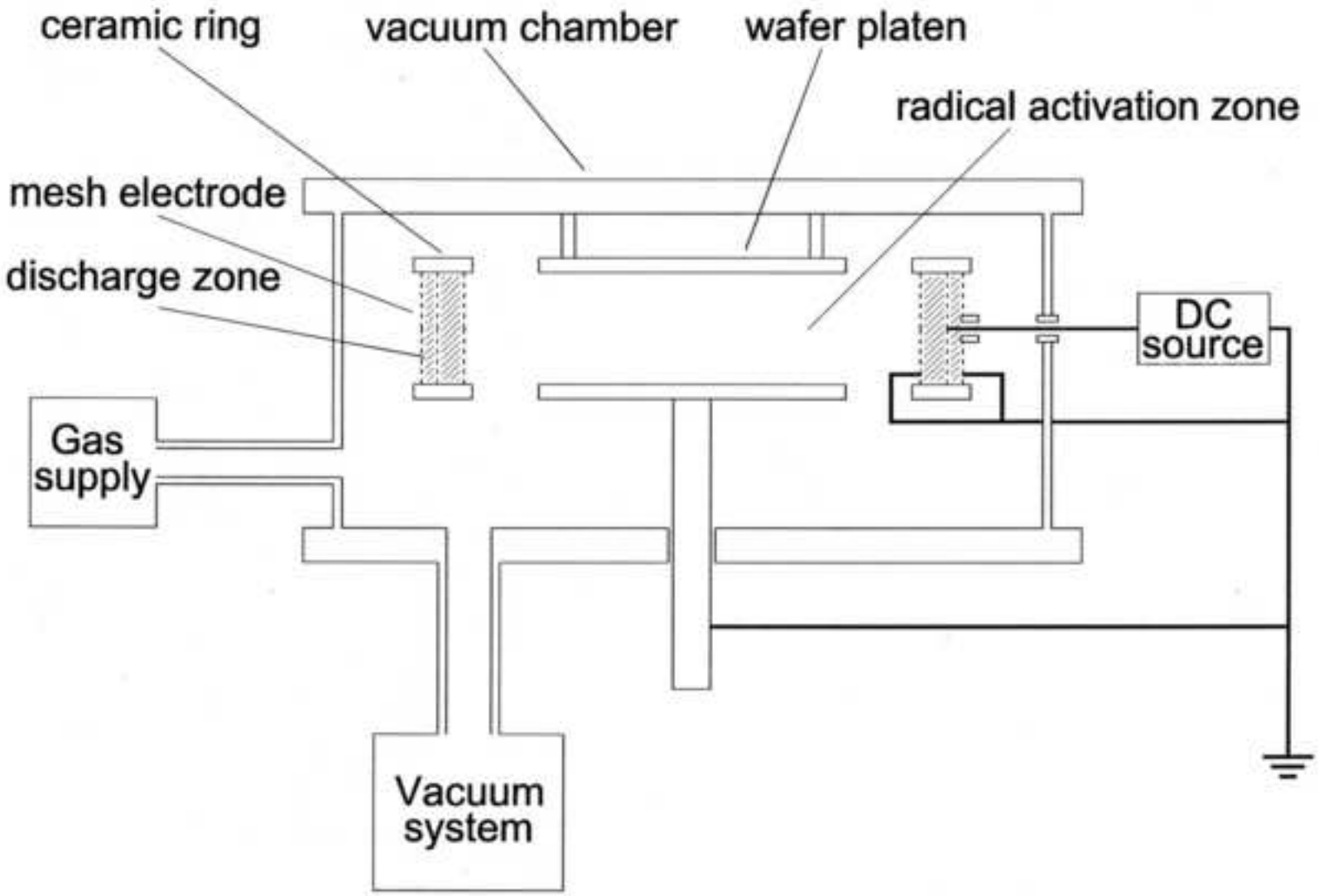
ceramic ring
vacuum chamber
wafer platen
radical activation zone
mesh electrode
discharge zone
DC source
Gas supply
Vacuum system

Figure 2

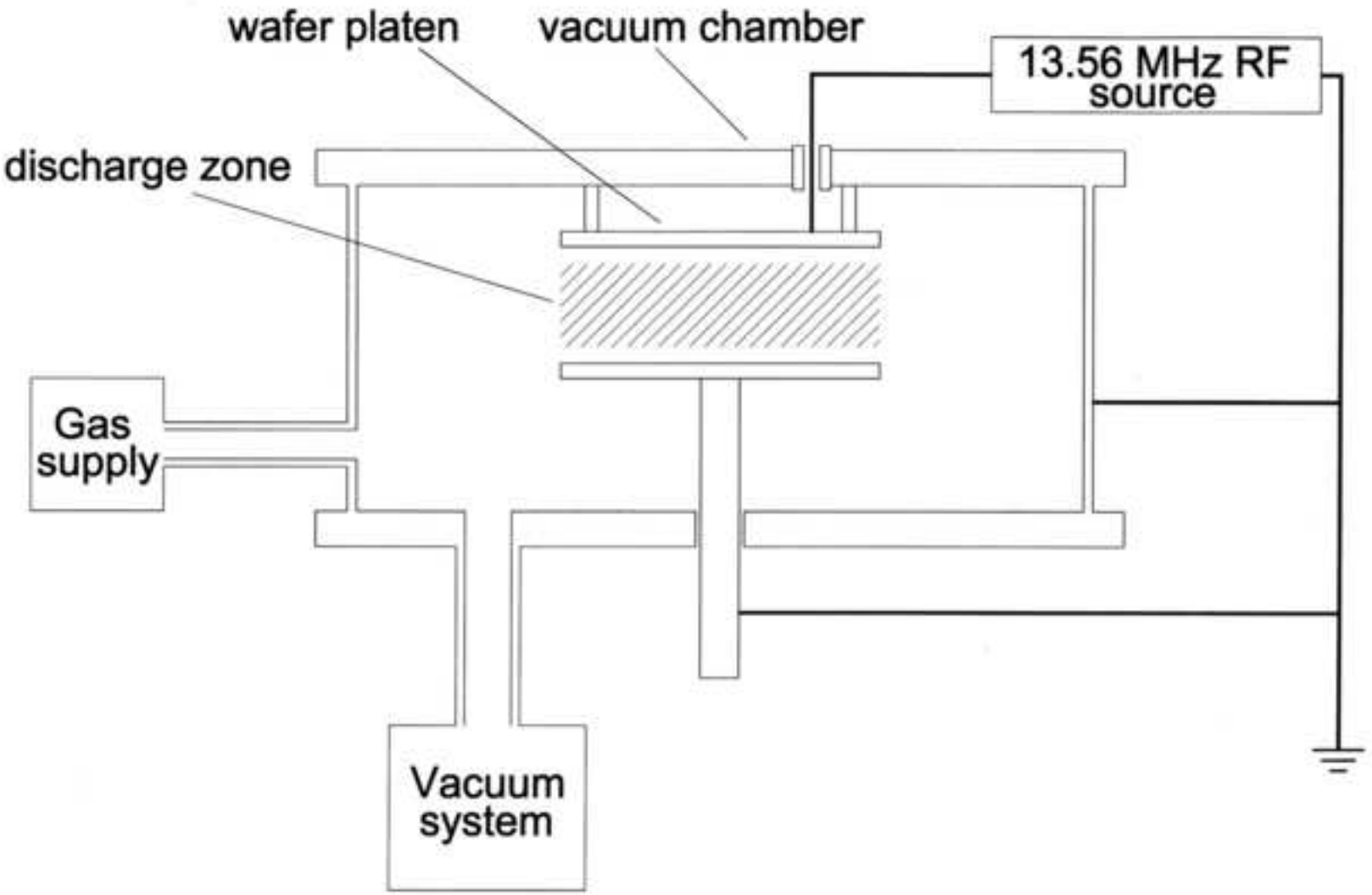
wafer platen
vacuum chamber
13.56 MHz RF source
discharge zone
Gas supply
Vacuum system

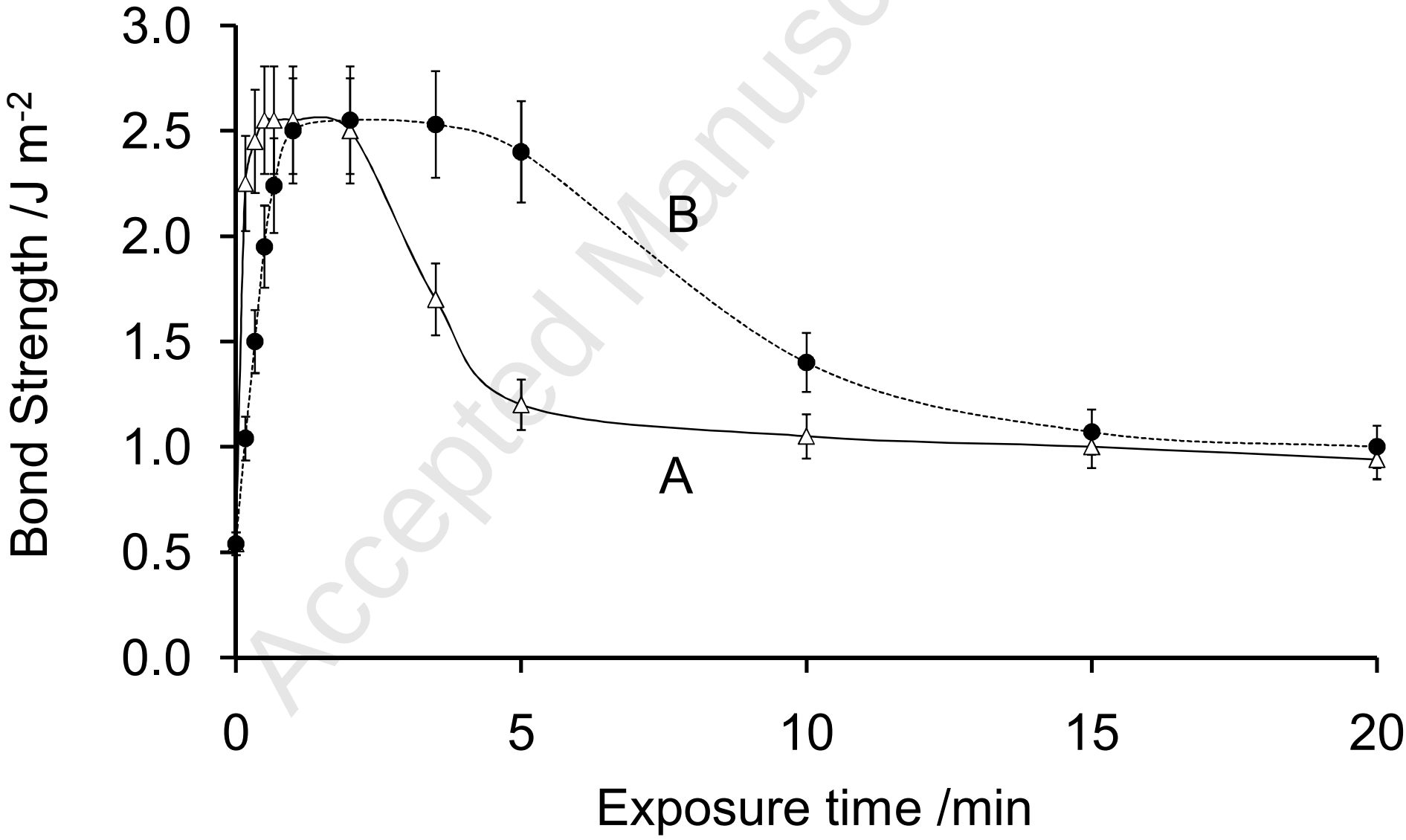

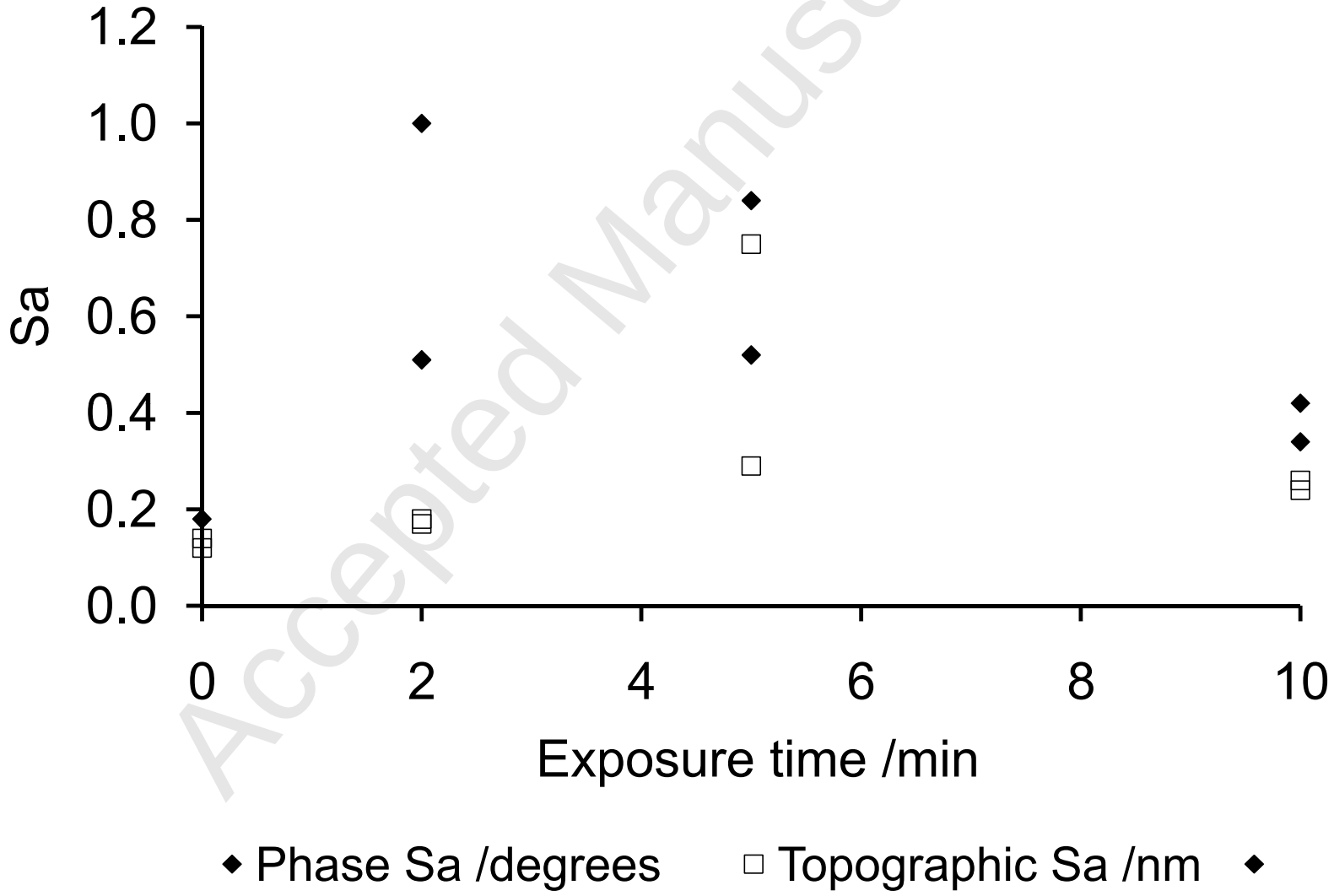

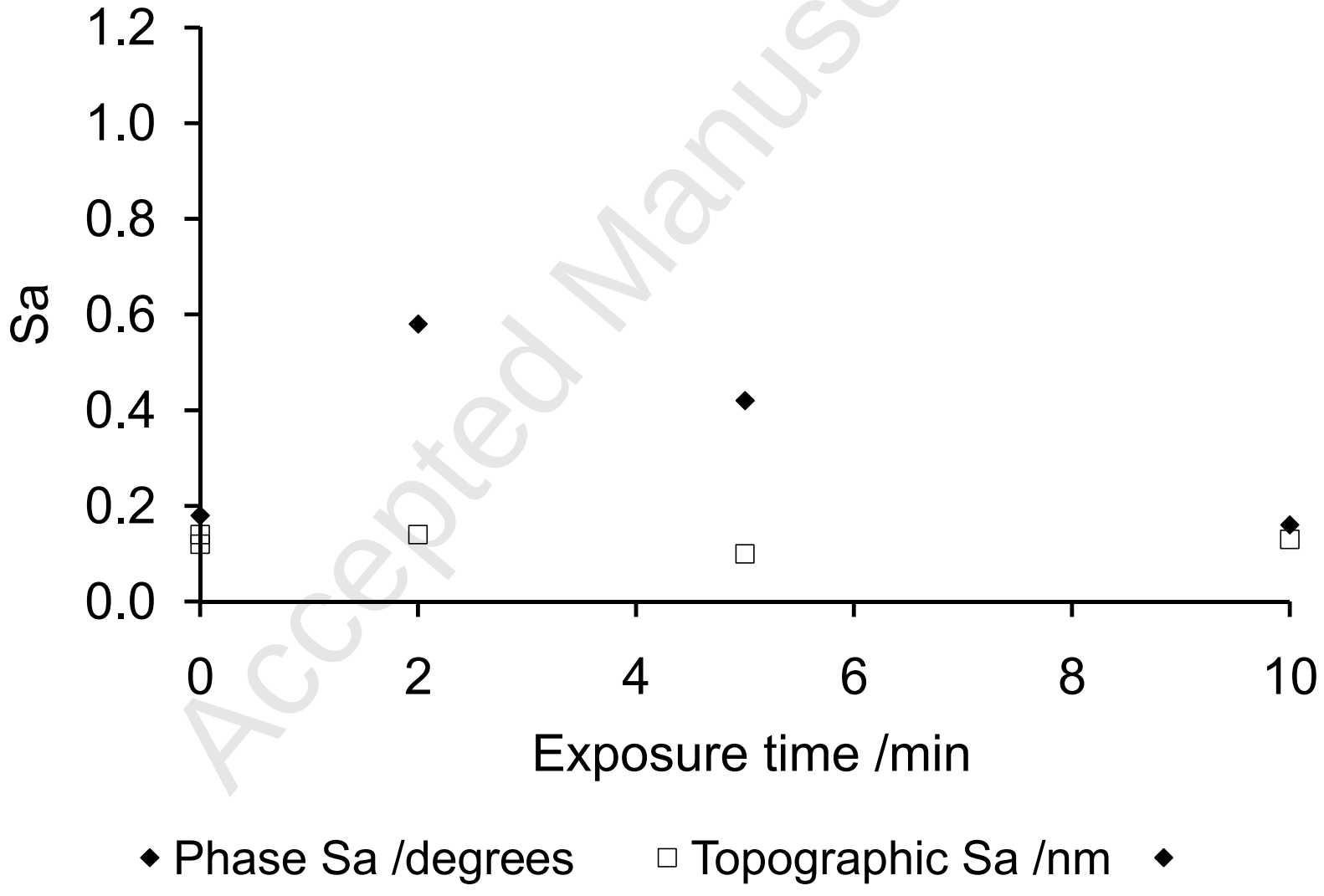

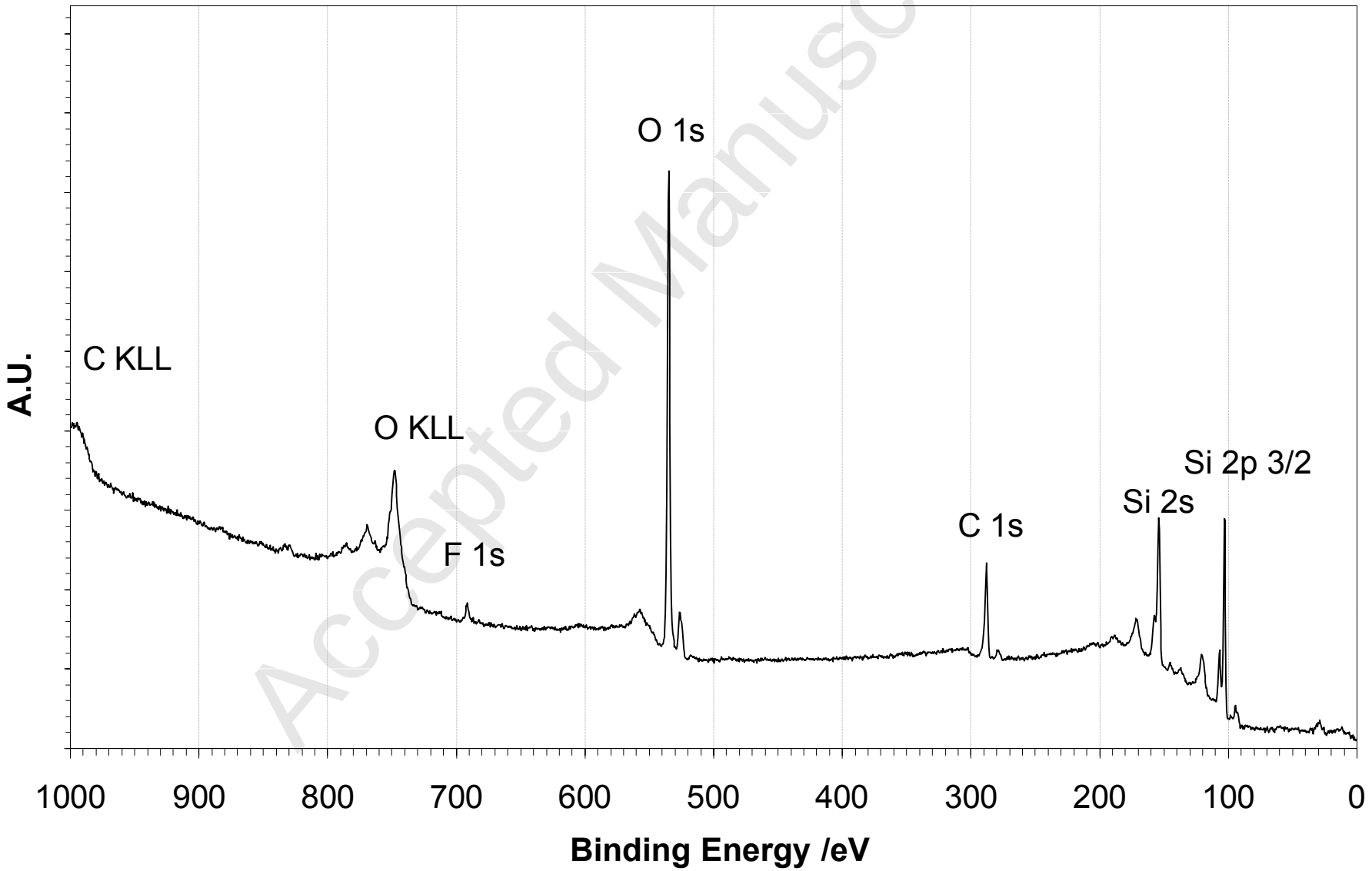

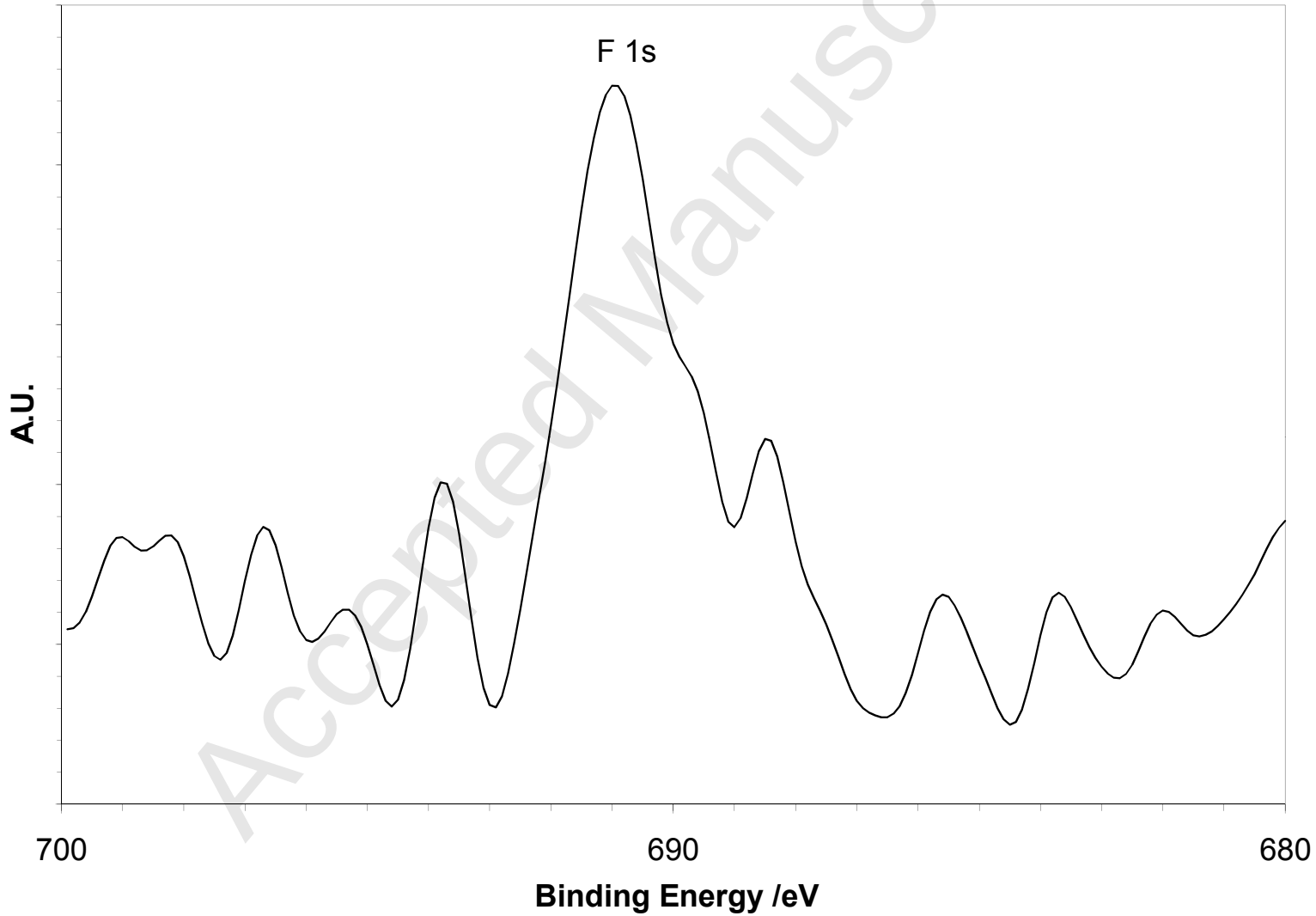

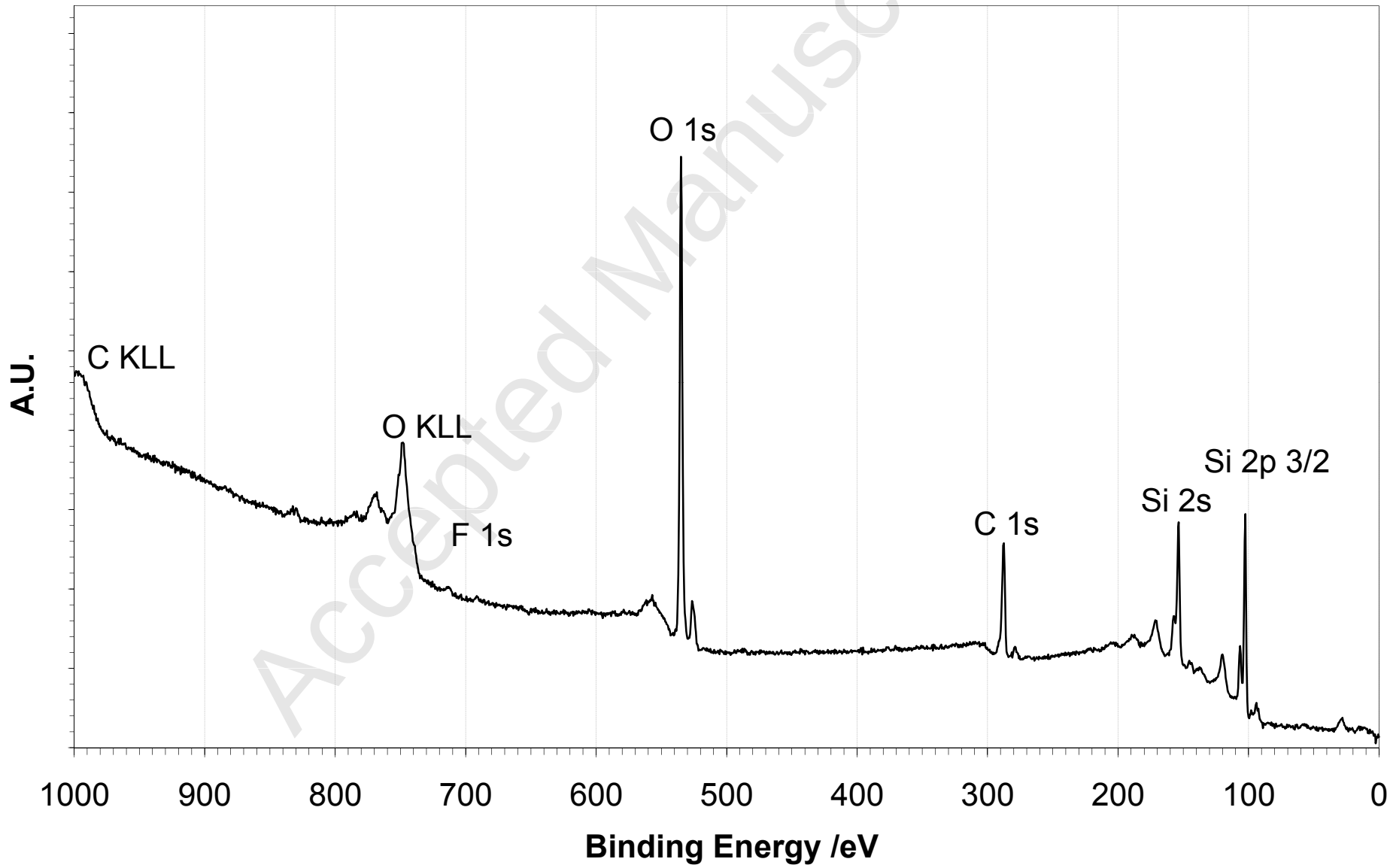

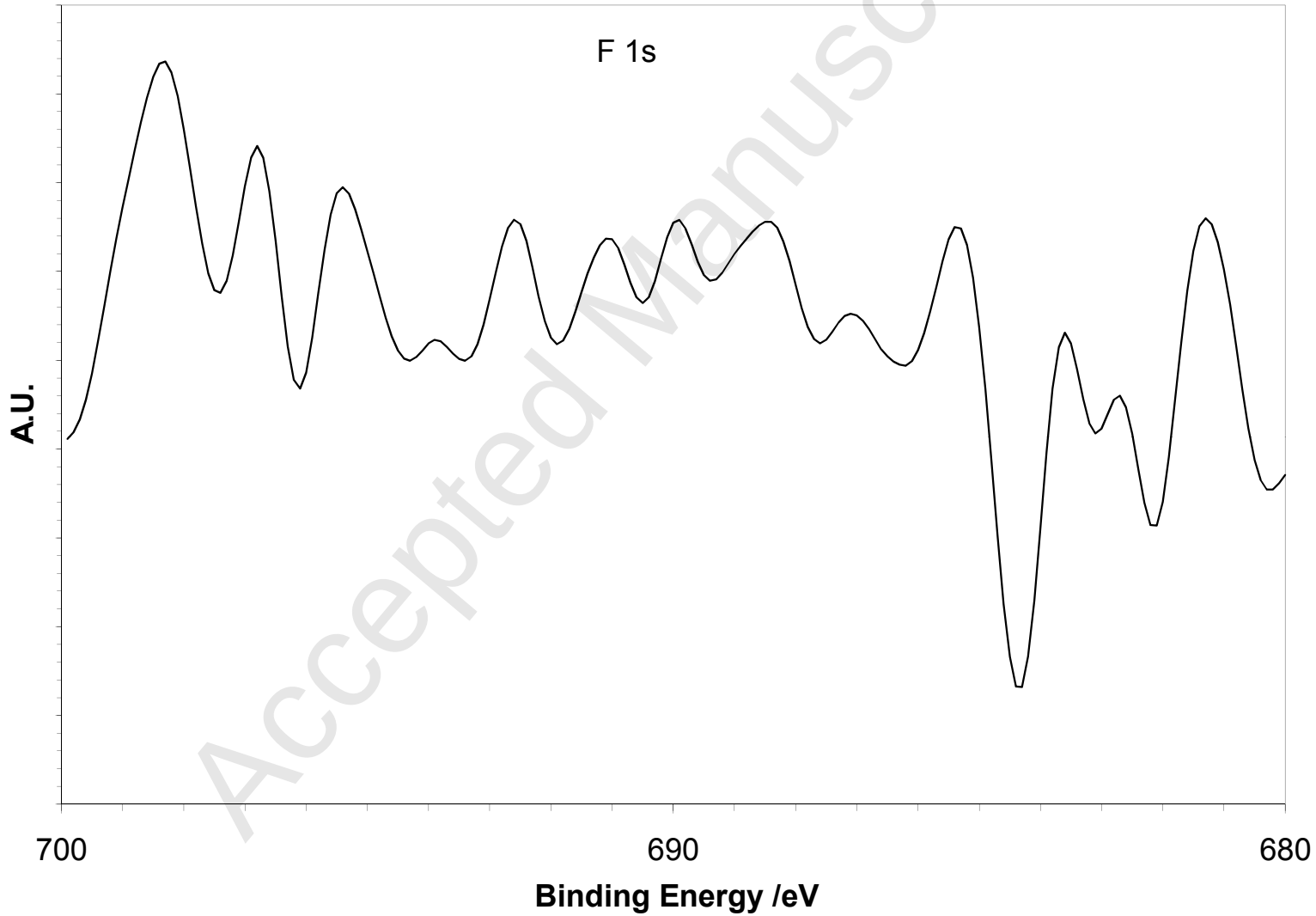

Figure 10

Figure 11

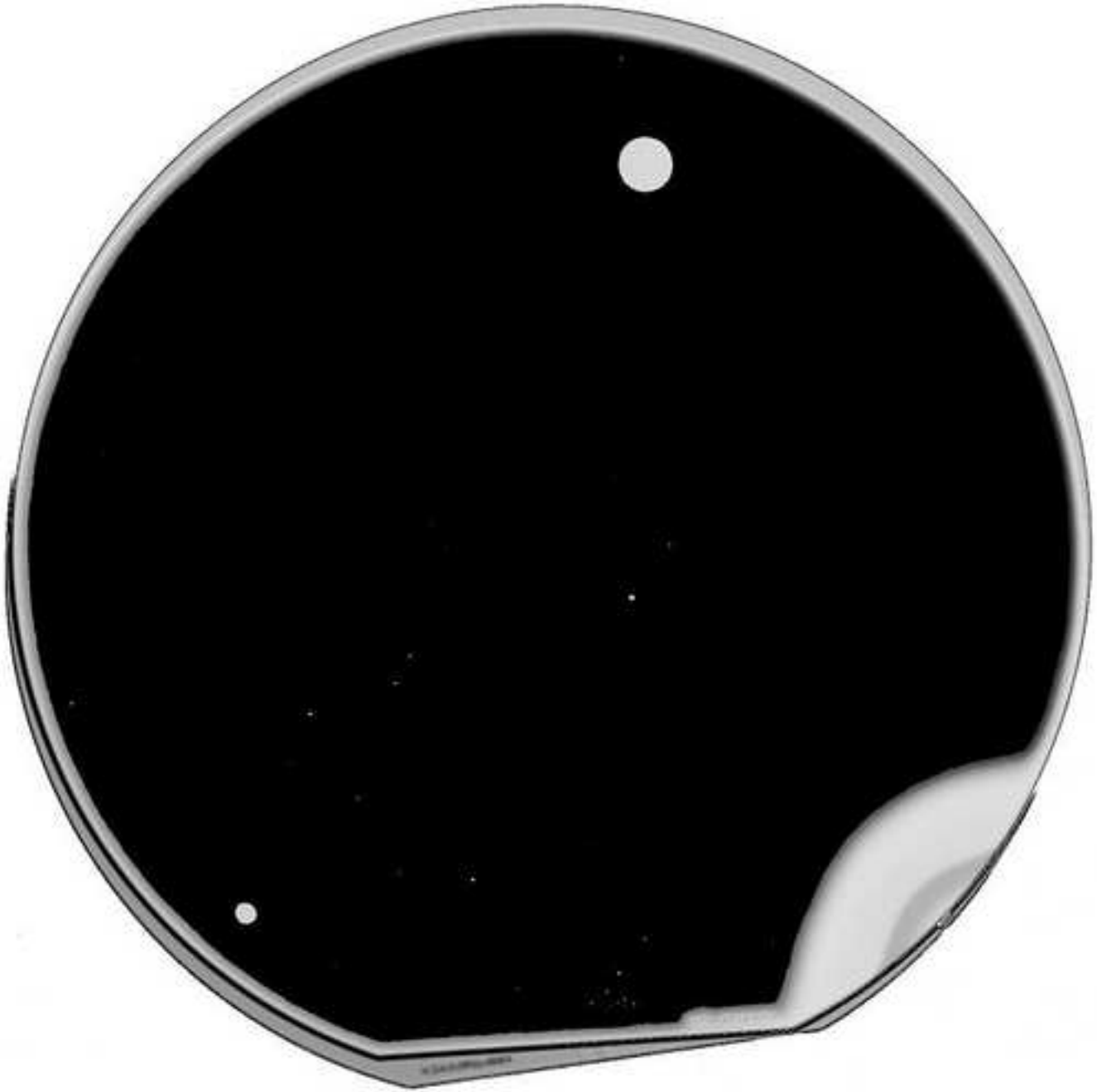

Figure 12